Self-Assembly of Supramolecular Triblock Copolymer Complexes

du Sart, Gerrit Gobius; Vukovic, Ivana; van Ekenstein, Gert Alberda; Polushkin, Evgeny; Loos, Katja; ten Brinke, Gerrit

Published in:
Macromolecules

DOI:
10.1021/ma902651t

2970 *Macromolecules* **2010**, *43*, 2970–2980
DOI: 10.1021/ma902651t

Macromolecules
ARTICLE

Self-Assembly of Supramolecular Triblock Copolymer Complexes

Gerrit Gobius du Sart, Ivana Vukovic, Gert Alberda van Ekenstein, Evgeny Polushkin, Katja Loos,* and Gerrit ten Brinke*

Laboratory of Polymer Chemistry, Zernike Institute for Advanced Materials, University of Groningen, Nijenborgh 4, 9747AG Groningen, The Netherlands

Received April 28, 2009; Revised Manuscript Received January 20, 2010

ABSTRACT: Four different poly(*tert*-butoxystyrene)-*b*-polystyrene-*b*-poly(4-vinylpyridine) (P*t*BOS-*b*-PS-*b*-P4VP) linear triblock copolymers, with the P4VP weight fraction varying from 0.08 to 0.39, were synthesized via sequential anionic polymerization. The values of the unknown interaction parameters between styrene and *tert*-butoxystyrene and between *tert*-butoxystyrene and 4-vinylpyridine were determined from random copolymer blend miscibility studies and found to satisfy $0.031 < \chi_{S,tBOS} < 0.034$ and $0.39 < \chi_{4VP,tBOS} < 0.43$, the latter being slightly larger than the known $0.30 < \chi_{S,4VP} \leq 0.35$ value range. All triblock copolymers synthesized adopted a P4VP/PS core/shell cylindrical self-assembled morphology. From these four triblock copolymers supramolecular complexes were prepared by hydrogen bonding a stoichiometric amount of pentadecylphenol (PDP) to the P4VP blocks. Three of these complexes formed a triple lamellar ordered state with additional short length scale ordering inside the P4VP(PDP) layers. The self-assembled state of the supramolecular complex based on the triblock copolymer with the largest fraction of P4VP consisted of alternating layers of P*t*BOS and P4VP(PDP) layers with PS cylinders inside the latter layers. The difference in morphology between the triblock copolymers and the supramolecular complexes is due to two effects: (i) a change in effective composition and, (ii) a reduction in interfacial tension between the PS and P4VP containing domains. The small angle X-ray scattering patterns of the supramolecules systems are very temperature sensitive. A striking feature is the disappearance of the first order scattering peak of the triple lamellar state in certain temperature intervals, while the higher order peaks (including the third order) remain. This is argued to be due to the thermal sensitivity of the hydrogen bonding and thus directly related to the very nature of these systems.

Introduction

Self-assembly of block copolymer-based systems continues to be one of the most studied subjects in polymer science due to the interesting physics and the wide range of potential technological applications.[1−5] Even more intriguing possibilities arise by combining block copolymer self-assembly with principles of supramolecular chemistry.[6] The most studied systems involve hydrogen bonded complexes between diblock copolymers and low molecular weight amphiphiles leading to noncovalent side-chain polymer architectures.[7−11] In the simplest case, one of the blocks is poly(4-vinylpyridine) (P4VP) with hydrogen bonded side chains consisting of phenols with a long alkyl tail, notably pentadecyl- (PDP) and nonadecylphenol (NDP). The phase separation in such systems occurs at two different length scales. First, the comb−coil diblock copolymer microphase separates into its two block phases, dictated by the volume fractions, interaction parameter and temperature (on a scale of tens to hundreds nanometers). Second, below ca. 60 °C, within the comb block, phase separation occurs between the alkyl tails of the amphiphile and the P4VP backbone (on a scale of 3−5 nm). Thus, hierarchical structure formation exists on two different length scales. Using a related but slightly more involved approach, different functional systems were obtained with, e.g., temperature-induced switching of proton conductivity and temperature-induced large photonic bandgap switching.[7,12]

Besides the possibility to introduce specific functional properties by selecting appropriate amphiphiles, an obvious additional advantage is that after the structure formation the amphiphiles may be removed by a simple washing step, e.g., using methanol or ethanol in the case of P4VP(PDP). Depending on the situation at hand, the large length scale morphology may survive the washing step, while a significant part of the original P4VP(PDP)-containing domains is now empty. In this respect it is of interest to note that for nominal fully complexed systems, i.e. one PDP molecule per 4VP unit, the amount of PDP is approximately three times as large as that of P4VP. This procedure has been used to create both nanoporous structures as well as nanorods.[13−16]

The creation of nanoporous structures remains an attractive research area due to the many applications foreseen. Quite often self-assembled pure diblock copolymers have been used,[17] with cylindrical[18] and gyroid morphologies[19,20] being the obvious structures of interest. For membrane-type devices, the minority phases are removed,[21,22] while the creation of, for example, photonic band gap materials may require the removal of the majority block.[23] Many of the studies presented in recent literature demonstrate the success in producing such nanoporous structures, although in several cases, it requires a significant effort to selectively remove one of the blocks of the original copolymer. Techniques that have been used, such as etching,[24,25] hydrolysis,[26] and ozonolysis,[27,28] are quite harsh and do not intrinsically ensure the survival of the morphology.

To obtain nanoporous thin films, the presence of a continuous network structure, e.g., gyroid morphology, is quite attractive because it does not require a specific orientation as is the case for a cylindrical morphology. So far, however, we have not been able to obtain self-assembled PS-*b*-P4VP(PDP) systems with network channels consisting of P4VP(PDP). This is one of the reasons why

*Corresponding authors. E-mail: (K.L.) k.u.loos@rug.nl; (G.t.B.) g.ten.brinke@rug.nl.

 Published on Web 02/18/2010

we turned our attention to ABC triblock copolymer-based supramolecules. The large number of parameters that may be varied for ABC triblock copolymers results in a vast array of self-assembled structures.[29] The triblock analogueies of the diblock morphologies, such as the triple alternating lamellar structure, alternating cylinders and core−shell cylinders are the simplest examples.[30−33] More fascinating possibilities arise when the A and C interface is favored, at which point so-called frustrated morphologies may be obtained.[34−38] For our studies, we were interested in having triblock copolymers with one of the blocks again being P4VP and which could be synthesized through anionic polymerization. Thus, poly(4-*tert*-butoxystyrene)-*b*-polystyrene-*b*-poly(4-vinylpyridine), P*t*BOS-*b*-PS-*b*-P4VP, was selected. Four different triblock copolymer systems were synthesized with P4VP weight fractions varying from 0.08 to 0.39. These triblock copolymers were found to self-assemble in the form of P4VP/PS core/shell cylinders in a matrix of P*t*BOS. The values of the interaction parameters involved, which were determined using random copolymer blend miscibility studies,[39,40] satisfied $0.031 < \chi_{S,tBOS} < 0.034$ and $0.39 < \chi_{4VP,tBOS} < 0.43$ and $0.30 < \chi_{S,4VP} \leq 0.35$, values that support the observation of core−shell morphologies.

When pentadecylphenol (PDP) is added, triblock copolymer-based supramolecules are formed due to the hydrogen bonding between PDP and P4VP (Figure 1).

This has two effects, it increases the volume fraction of the P4VP block and it reduces the interfacial tension between PS and P4VP.[41] The amount of PDP amphiphile is an easily adjustable parameter. However, in the present paper we will focus on triblock copolymer complexes with a nominal amount of PDP, i.e., one PDP molecule per 4VP repeat units. Three out of the four supramolecular systems were found to self-assemble into a triple lamellar morphology, whereas for the system with the highest fraction of P4VP the ordered state consisted of alternating thin P*t*BOS layers and thick P4VP(PDP) layers containing PS cylinders. To obtain self-assembled states with P4VP(PDP) continuous networks, smaller amounts of PDP are required, as will be discussed in a future paper.

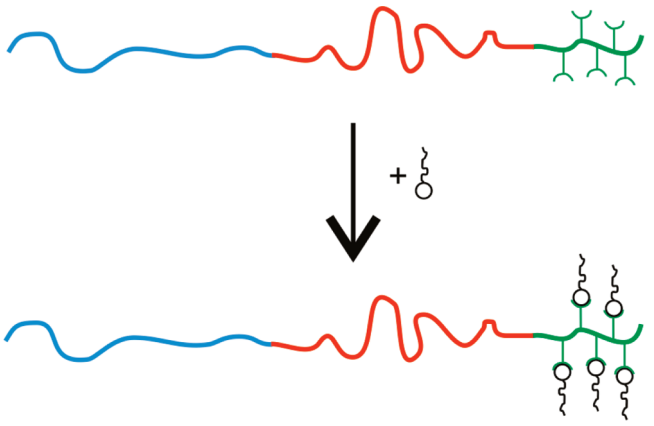

Figure 1. Schematic representation of the formation of triblock copolymer−amphiphile supramolecules.

Experimental Section

Materials. *sec*-Butyllithium (sBuLi, Aldrich, 1.4 M in cyclohexane) was used without further purification. Styrene (St, 99%, Acros) was stirred for 24 h under nitrogen atmosphere over CaH_2. It was then condensed at room temperature (10−6 mbar) into a flask containing dibutylmagnesium. After stirring overnight, it was condensed a second time into a storage ampule, which was kept at 6 °C under nitrogen atmosphere. 4-Vinylpyridine (4VP, Aldrich, 95%) was dried under nitrogen atmosphere over calcium hydride for 48 h and condensed into a flask containing freshly cut sodium. After stirring overnight at room temperature, it was condensed into an ampule and stored under nitrogen at −18 °C. 4-*tert*-Butoxystyrene (tBOS, Aldrich, 99%) was distilled twice from CaH_2 and stored at 6 °C. Tetrahydrofuran (THF, Acros, 99 +%) was first distilled over a potassium/sodium alloy and then condensed and subjected to three freeze−thaw cycles. It was reacted with *tert*-butyllithium for 15 min at −78 °C during which a yellow color indicated that the solvent was suitable for anionic polymerization. Finally the solvent was condensed into the polymerization flask. LiCl (Aldrich, 99.99 +%) was dried overnight in vacuum at 130 °C. Chloroform (p.a., LAB-SCAN) was used as received. 3-Pentadecylphenol (PDP, 98%, Aldrich) was recrystallized twice from petroleum ether. The free radical initiator α,α′-azoisobutyronitrile (AIBN, Fluka, ≥ 98.0%) was used as received. DMF and toluene were distilled and stored under nitrogen atmosphere. Methanol was degassed by bubbling dry nitrogen through it for 1 h at room temperature.

Anionic Polymerization of PtBOS-*b*-PS-*b*-P4VP. The PtBOS-*b*-PS-*b*-P4VP linear triblock copolymers were synthesized through a three-step sequential anionic polymerization in THF at −78 °C (Scheme 1).

All anionic polymerizations and purification techniques were performed on a high-vacuum line. At room temperature, 800 mL of THF was condensed into a 1000 mL flask containing LiCl in 5-fold excess relative to the later introduced amount of initiator. After three freeze−thaw cycles, a few drops of *t*BOS were added and the solution was titrated with *s*BuLi until the solution just turned slightly yellow. The solution was now

Scheme 1. Synthesis Route of the P*t*BOS-*b*-PS-*b*-P4VP Triblock Copolymers

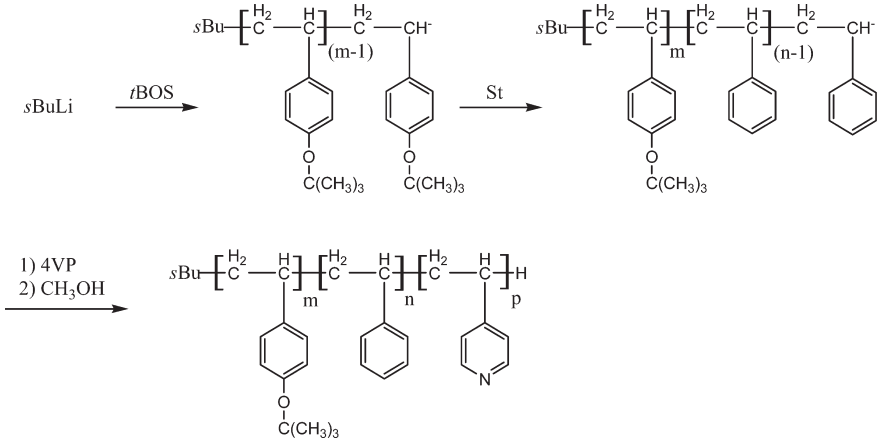

Table 1. Triblock Copolymer Properties

	weight fractions				
entry	P*t*BOS	PS	P4VP	M_n[a] (kg/mol)	PDI
1	0.46	0.46	0.08	76.0	1.04
2	0.29	0.56	0.15	49.7	1.07
3	0.34	0.34	0.32	13.3	1.06
4	0.24	0.38	0.39[b]	90.6	1.09

[a] On the basis of the reaction stoichiometry and the molecular weight of the PtBOS precursor as determined by GPC. [b] Fractions do not add up to 1 because of rounding-off errors.

cooled to −78 °C, and the calculated amount of *t*BOS was added with a degassed syringe. Next, the calculated amount of *s*BuLi was added and the polymerization was allowed to proceed for 45 min. Then a 10 mL sample was withdrawn for GPC analysis and dispersed into degassed methanol. After this, the polymerization of styrene was started by adding the calculated amount to the reaction mixture. Again, after 45 min, a GPC sample was withdrawn and precipitated in methanol. Now the calculated amount of 4VP was added and the polymerization was allowed to proceed for another hour. The polymerization was stopped by the addition of 5 mL of degassed methanol. The polymers were precipitated in methanol (low fractions of P4VP) or cold hexane (higher fractions of P4VP). The molecular weights and polydispersities were determined by GPC in DMF.

Triblock Copolymer Complexes with PDP. The triblock copolymers (100−200 mg) were dissolved in chloroform together with the calculated amount of PDP. After at least 2 h of stirring at room temperature, the solution was poured into a glass Petri dish, which was subsequently placed into a saturated chloroform atmosphere. After at least a week of solvent annealing, the dish was heated shortly (10 min) in an oven of 130 °C to erase any solvent history. Bulk triblock copolymer films were made by dissolving the polymer in chloroform and applying the procedure just mentioned. After solvent annealing, these films were heated shortly at a temperature of 180 °C. NMR confirmed that no residual solvent was left in the samples.

Characterization. Gel permeation chromatography (GPC) measurements were performed in DMF with 0.01 M LiBr at 70 °C (1 mL/min) on a Waters 600 Powerline system, equipped with 2 columns (PL-gel 5 μ, 30 cm mixed-C, Polymer Laboratories) and a Waters 410 differential refractometer. The GPC was calibrated using narrow disperse polystyrene standards (Polymer Laboratories).

Bright-field transmission electron microscopy (TEM) was performed on a JEOL-1200EX transmission electron microscope operating at an accelerating voltage of 100 kV. To prepare TEM samples, piece of film was embedded in an epoxy resin (Epofix, Electron Microscopy Sciences) and cured overnight at 40 °C. The sample was subsequently microtomed to a thickness of about 70 nm using a Leica Ultracut UCT-ultramicrotome and a Diatome diamond knife at room temperature. The microtomed sections were floated on water and subsequently placed on copper grids. To obtain contrast during TEM, the samples were stained with iodine (3 h) or RuO_4 (100 min).

^{1}H NMR spectra in $CDCl_3$ were recorded on a 300 MHz Varian VXR operating at room temperature. Small-angle X-ray scattering (SAXS) measurements were performed at the Dutch−Belgian Beamline (DUBBLE) at ESRF in Grenoble, France. The sample−detector distance was about 7.3 m, while the X-ray wavelength was 1.24 Å (E = 10 keV). The scattering vector q is defined as $q = (4\pi/\lambda)\sin\theta$, where θ is half of the scattering angle.[42] The samples were investigated during a heating−cooling−heating sequence in the range of 20−200 °C, employing a heating (cooling) rate of 10 °C/min. Data were collected during 30 s per frame.

(Temperature-modulated) differential scanning calorimetry (M-DSC) was performed with a TA Instruments Q1000. A modulated mode with heating/cooling rate of 1 °C/min, an amplitude of 0.5 °C and a period of 60 s was used.

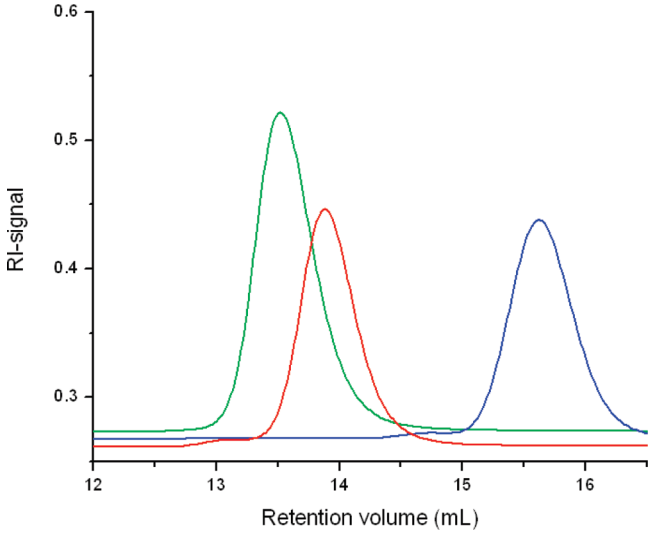

Figure 2. GPC elution diagrams for the three successive polymerization steps of P*t*BOS-*b*-PS-*b*-P4VP (entry **2** in Table 1; M_n = 49.7 kg/mol, f_{tBOS} = 0.29, f_{St} = 0.56, f_{4VP} = 0.15). The blue curve represents the homopoly(*t*BOS) precursor, the red line represents the P*t*BOS-*b*-PS precursor and the green line represents the final P*t*BOS-*b*-PS-*b*-P4VP triblock copolymer.

Results and Discussion

The PtBOS-*b*-PS-*b*-P4VP linear triblock copolymers were synthesized through a three-step sequential anionic polymerization. For each polymerization step well-defined polymers with a low polydispersity index (PDI) and predictable molecular weights were obtained. Table 1 lists the properties of the four different triblock copolymers synthesized.

The controlled nature of the reaction is supported by the GPC elution diagrams. A representative example is shown in Figure 2. The elution peaks are symmetrical around their elution volume and each peak is completely shifted toward lower elution volumes after each polymerization step. For the triblock copolymer with a very low fraction of 4VP (entry **1** in Table 1), precipitation in methanol was possible, but for higher fractions, cold hexane was used as the nonsolvent for precipitation.

Triblock Copolymer Morphologies. To understand the self-assembly of the P*t*BOS-*b*-PS-*b*-P4VP triblock copolymer systems it is important to know the values of the three different interaction parameters involved. For PS and P4VP the inequality $0.30 < \chi_{S,4VP} \leq 0.35$ was determined some years ago using a random copolymer miscibility study.[39] This value was later confirmed by a small-angle X-ray scattering study on disordered PS-*b*-P4VP diblock copolymers.[43] For the other two parameters a similar random copolymer miscibility study was performed, which led to the conclusion that they satisfied the following inequalities: $0.031 < \chi_{S,tBOS} < 0.034$ and $0.39 < \chi_{4VP,tBOS} < 0.43$.[40] Because $\chi_{4VP,S} \gg \chi_{S,tBOS}$ and $\chi_{4VP,tBOS} \geq \chi_{4VP,S}$ it comes as no surprise that all four triblock copolymer systems adopted a core−shell cylindrical self-assembled morphology in which the PS/P4VP interface is minimized at the cost of creating a larger P*t*BOS/PS interface. As a representative example, block copolymer **2** (f_{tBOS} = 0.29, f_{St} = 0.56, f_{4VP} = 0.15) will be discussed. When staining with iodine, only the P4VP phase is stained and hexagonally ordered cylinders are observed (Figure 3a). When staining with ruthenium tetroxide (Figure 3b), all three phases are stained, but the P*t*BOS

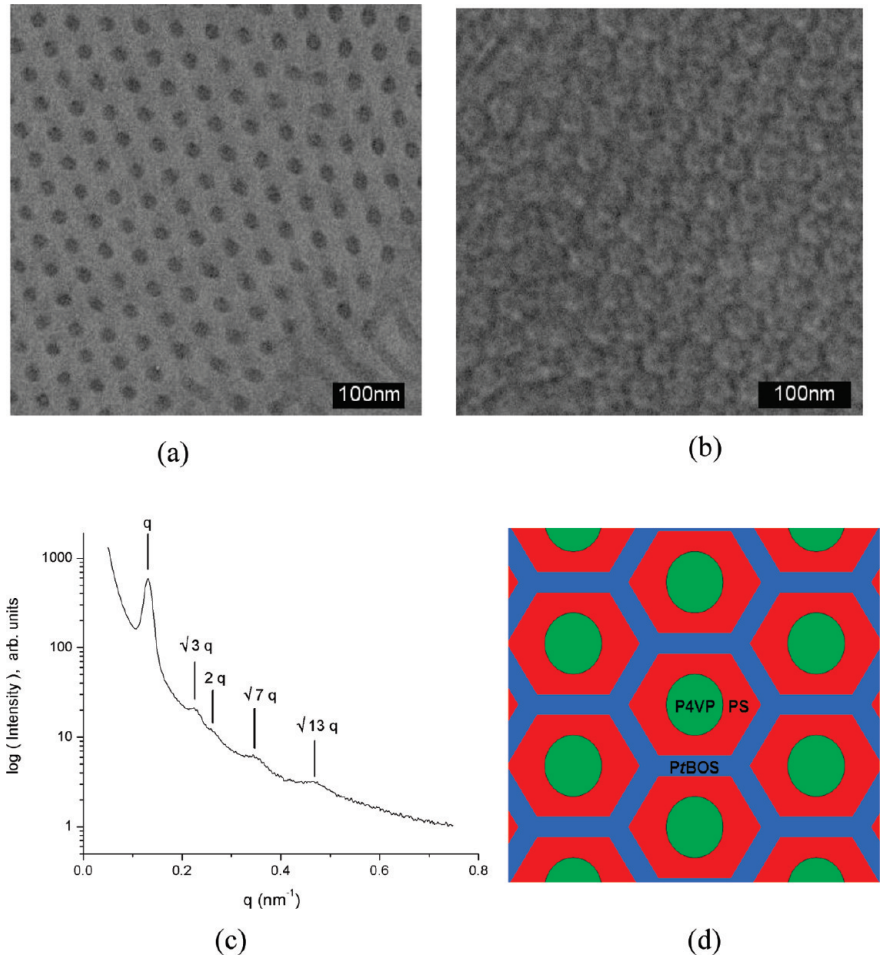

Figure 3. Bright-field TEM image of entry **2** in Table 1, stained with iodine (a) and stained with iodine and ruthenium tetroxide (b), the corresponding SAXS intensity profile at room temperature (c), and a schematic representation of the morphology (d). Green represents P4VP, red is PS, and blue is P*t*BOS.

and P4VP phases more heavily than the PS phase. On the basis of these two staining methods it is clear that a core−shell cylindrical self-assembled morphology is formed. The shell (consisting of the PS block) seems to have a hexagonal shape, which has been already reported for tri- and tetrablock copolymer systems.[44,45] Gido and co-workers[46] observed a similar self-assembly for a linear polyisoprene-*b*-polystyrene-*b*-poly(2-vinylpyridine) triblock copolymer. The nonconstant mean curvature interface was explained to be due to the packing of the chains in relation to the relative block lengths.[46]

Entry 3 ($f_{tBOS} = f_{St} = 0.34, f_{4VP} = 0.32$) is the triblock copolymer with the lowest molecular weight (about 5 kg/mol per block). SAXS again revealed a cylindrical morphology. It is actually quite interesting that the self-assembled state of this particular triblock copolymer consists of three microphases. The phase separation of P4VP from PS and P*t*BOS is not a surprise, given the large values of the Flory−Huggins interaction parameters $\chi_{S,4VP}$ and $\chi_{tBOS,4VP}$. However, since $0.031 < \chi_{S,tBOS} < 0.034$, such low molecular weights could well have resulted in a mixed PS/P*t*BOS phase. And indeed, a mixed state was found for the diblock precursor of this polymer as demonstrated by its SAXS scattering pattern presented in Figure 4. Because of the small contrast between PS and P*t*BOS and the fact that we are far from criticality, not even a correlation hole peak is visible.

Apparently, the triblock copolymer architecture results in segregation between the P*t*BOS and PS blocks once the P4VP blocks are segregated. This phenomenon has been described before by Chatterjee et al.[47] for poly(isoprene)-*b*-polystyrene-*b*-poly(ethylene oxide) triblock copolymers. They observed that a symmetric IS diblock precursor ($f_I = 0.51, f_{St} = 0.49$, and $M_n = 6.9$ kg/mol) was in the disordered state, while the corresponding triblock copolymer ($f_I = 0.28$, $f_{St} = 0.24, f_{EO} = 0.48$, and $M_n = 14.2$ kg/mol) showed a nearly completely segregated three domain structure. The interaction parameter for the isoprene and styrene block satisfies $\chi_{IS} = 0.034$, which fortuitously corresponds almost precisely to our situation where $0.031 < \chi_{S,tBOS} < 0.034$.

Summarizing, we see that the core−shell cylindrical structure is stable for a wide range of P4VP fractions. This kind of behavior is supported by a study of Tang et al.,[48] who performed a real space implementation of the self-consistent field theory in a two-dimensional space. They found that for ABC triblock copolymers with $\chi_{AB}N \ll \chi_{BC}N$ and $\chi_{BC}N$ slightly smaller than $\chi_{AC}N$(which corresponds perfectly to our case), the core−shell cylindrical morphology is found for a large part of the ternary phase diagram.

Morphology of the Triblock Copolymer-Based Supramolecules. The triblock copolymers were subsequently complexed with a nominal amount of PDP, i.e., one PDP molecule per 4-pyridine unit. The weight fractions and molecular weights of the complexes investigated are listed in Table 2.

In the microphase-separated self-assembled states that will be discussed, most of the PDP, but not all,[49] will actually reside in the P4VP containing domains. In particular some PDP will be present in the PS domains. At elevated

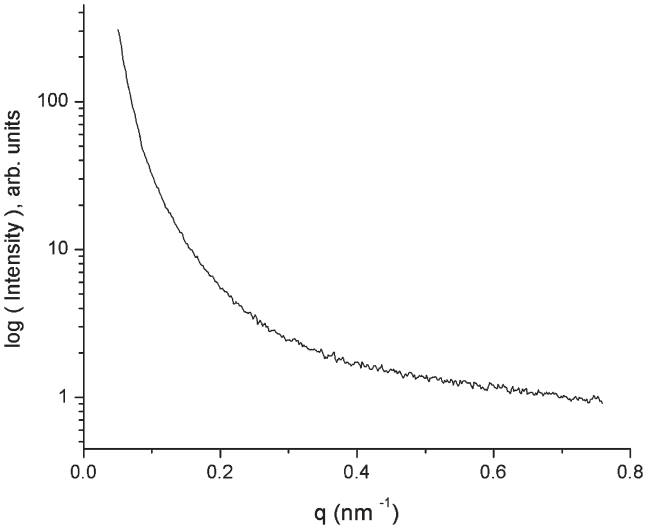

Figure 4. SAXS scattering intensity profile for the P*t*BOS-*b*-PS precursor ($f_{tBOS} = f_{St} = 0.50$, $M_n = 9.0$ kg/mol) of triblock copolymer **3** (Table 1).

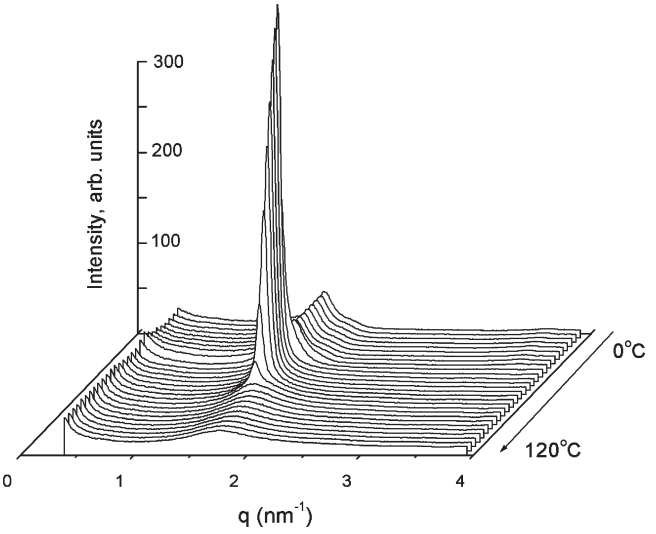

Figure 5. SAXS intensity scattering patterns of P*t*BOS-*b*-PS-*b*-P4VP-(PDP)$_{1.0}$ as a function of temperature, demonstrating the short-length-scale ordering peaks in the range of $q = 1.7$ nm^{-1}.

Table 2. Properties of P*t*BOS-*b*-PS-*b*-P4VP(PDP)$_{1.0}$ Supramolecules

	weight fractions			
entry	P*t*BOS	PS	P4VP(PDP)$_{1,0}$	M_n[b] (kg/mol)
1	0.37	0.37	0.25[a]	93.4
2	0.16	0.50	0.33[a]	87.6
3	0.17	0.17	0.65[a]	26.0
4	0.11	0.18	0.71	192.0

[a] Fractions do not add up to 1 because of rounding-off errors. [b] Calculated as the sum of the mass of the PDP molecules and the M_n of the triblock copolymers.

temperatures (>120 °C) PDP becomes even miscible with homopolymer PS. In contrast, a mixture of PDP and homopolymer P*t*BOS remains macrophase separated up to temperatures as high as 200 °C. Hence, on heating the self-assembled P*t*BOS-*b*-PS-*b*-P4VP(PDP) systems, it is expected that PDP will gradually diffuse into the PS phase and probably not, or far less, into the P*t*BOS phase. Even so, due to the favorable hydrogen bonding, most PDP will remain inside the P4VP-containing domains.

Complex Formation. It is well-known that hydrogen-bonded complexes of poly(4-vinylpyridine) with PDP form a microphase separated lamellar morphology below ca. 60 °C.[50,51] The pentadecyl chains separate from the polymer and the phenol groups of PDP. This results in a lamellar arrangement with a period of about 3−5 nm, depending on the amount of PDP and the temperature. To prove the existence of this internal short-length-scale structure in the triblock copolymer-based supramolecules, a series of SAXS profiles were recorded at scattering angles corresponding to this small length scale. As an example, SAXS curves of complex **4** as a function of temperature are presented in Figure 5.

A number of features can be observed that are well-known from our previous research on homopolymer-based P4VP-(PDP) and diblock copolymer-based PS-*b*-P4VP(PDP).[50−52] Above room temperature a peak that indicates a lamellar microphase separated morphology of P4VP and the alkyl tails of PDP is found at about $q = 1.7$ nm^{-1} (there is a small temperature dependence). The length scale that corresponds to this peak is about 3.7 nm. This value is in good agreement with the length scales known from previous PS-*b*-P4VP(PDP) studies. Upon heating, this peak disappears and changes into a correlation hole peak; the temperature at which this occurs is the order−disorder temperature (ODT) for the small length scale. Although hydrogen bonding is thermally reversible, up to high temperatures many hydrogen bonds remain and the homogeneously mixed state consists of P4VP(PDP) hydrogen-bonded side-chain polymers and some free PDP.[53] Using DSC, the transition temperature for this particular sample was found to be 78 °C upon heating and 73 °C upon cooling. The ODTs of the microphase separation in the P4VP(PDP) domains of all four complexes studied are in the same range of temperature. In the case of homopolymer P4VP with an equimolar amount of PDP the ODT is approximately 60 °C, a value which is also found for the PS-*b*-P4VP(PDP)$_{1,0}$ diblock copolymer-based systems.[52]

Compared to these systems, our triblock copolymer complexes show a somewhat higher ODT of the small length scale structure, for which we have no clear explanation at the moment. Below room temperature crystallization of the alkyl tails of PDP occurs. This results in a "collapse" of the lamellar structure, as is reflected by a shift in the peak position to $q = 1.88$ nm^{-1} at 10 °C. The corresponding length scale of 3.3 nm is somewhat smaller. Besides a shift in peak position, crystallization is also accompanied by a strong reduction in the intensity of the scattering peak.

Self-Assembly of the Triblock Copolymer (PDP)$_{1.0}$ Complexes. As revealed by TEM (Figure 6) for complex **1** of Table 2, the cylindrical morphology of the pure triblock copolymer (entry **1** from Table 1) turns into a triple lamellar structure after addition of a nominal amount of PDP. The iodine stained sample shows relatively thin P4VP(PDP) layers, whereas staining with ruthenium tetroxide also reveals the PS and P*t*BOS layers.

As presented in Table 2, the block weight fractions of complex **1** satisfy P*t*BOS:PS:P4VP(PDP) = 0.37:0.37:0.25 if it is assumed that all PDP is hydrogen bonded to P4VP. In reality the weight fraction of in particular the PS-containing domains will be somewhat larger due to the presence of some PDP inside the PS layers. The presence of a triple lamellar morphology does not come as a real surprise. The comb copolymer architecture of the P4VP(PDP) block requires more space at the interface compared to a linear architecture

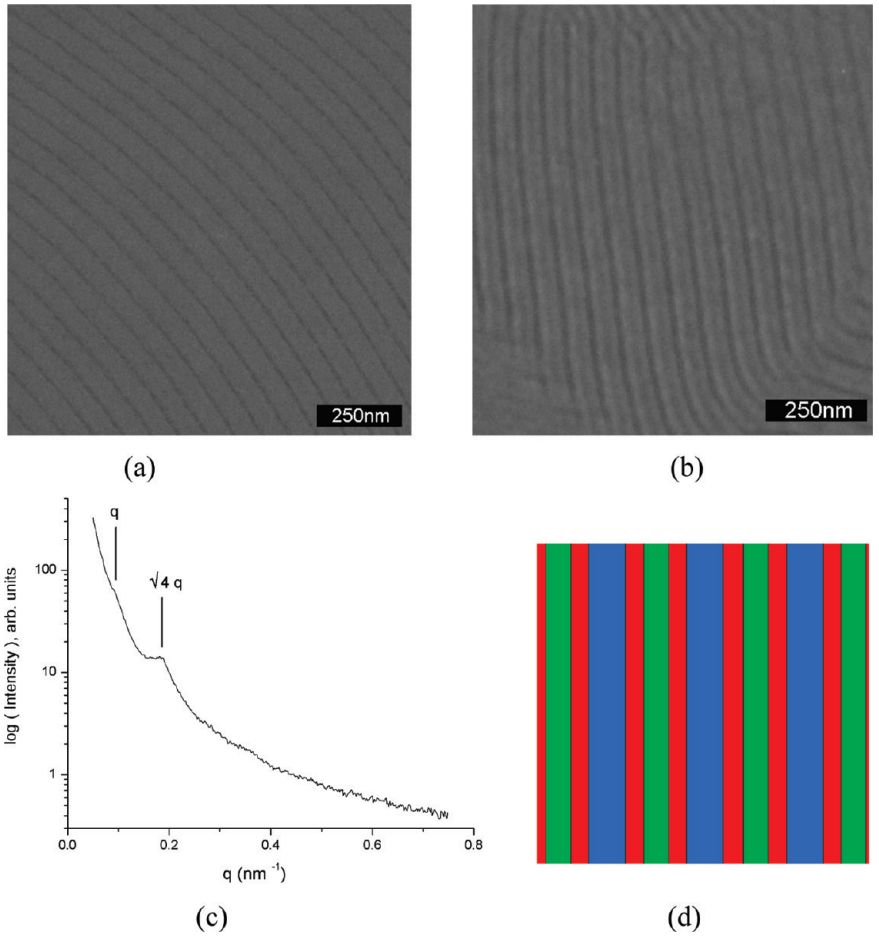

Figure 6. Bright-field TEM image of complex **1** (Table 2), stained with iodine (a) and stained with ruthenium tetroxide (b), the corresponding SAXS intensity profile at room temperature (c), and a schematic representation of the morphology (d). Green represents P4VP(PDP), red is PS, and blue is P*t*BOS. The additional short length scale ordering in the P4VP(PDP) layers is not indicated.

thus promoting the lamellar morphology. In general, blocks which require extra space such as graft or star[54] blocks show a tendency to form lamellar self-assemblies for a large part of the phase diagram. Furthermore, the interface tension between PS and P4VP(PDP) is reduced considerably compared to pure PS and P4VP.[41] The long period, as derived from the TEM images is 68 ± 2 nm, in good agreement with 66.1 nm found from SAXS measurements (Figure 6c).

Similar behavior is observed for complex **2**. While the original triblock copolymer also self-assembles into core−shell cylinders, upon addition of one PDP molecule per P4VP unit, a triple lamellar structure is found for the complex as demonstrated by both TEM and SAXS (Figure 7). From the first order SAXS peak (q = 0.117 nm^{-1}) the long period is found as d = 53.7 nm, compared to 46 ± 2 nm measured directly from TEM.

Complex 3 has a composition given by $f_{tBOS} = f_{St}$ = 0.17, $f_{4VP(PDP)}$ = 0.65, and a relatively low molecular weight of only 26.0 kg/mol. SAXS did not show any indication of microphase separation. Although some regions with a tendency to form lamellar phases could be found in the TEM picture, the sample as a whole appeared mostly in a disordered state. Not surprisingly, upon addition of PDP, the interaction parameter between PS and P4VP(PDP) as compared to that between PS and pure P4VP is lowered to such an extent that phase separation no longer occurs.

Finally, for complex **4**, the composition satisfies f_{tBOS} = 0.11, f_{St} = 0.18, $f_{4VP(PDP)}$ = 0.71. Now a structure is found in which P*t*BOS forms very thin lamellae between thick P4VP(PDP) layers containing PS cylinders (Figure 8). Besides the familiar lamellar structure peaks, the SAXS pattern also contains a $\sqrt{6}$ peak. The lamellar period, as measured from the TEM images is 60 ± 3 nm, while SAXS gives 66.1 nm. This is the first example of a frustrated morphology for our systems, since the P4VP(PDP) domains not only have an interface with polystyrene, but also with P*t*BOS. Apparently, the system foremost wants to minimize the PS/P*t*BOS interactions. Because of the presence of PDP the interaction between PS and P4VP(PDP) is less unfavorable. The phase behavior of this particular system, as demonstrated by SAXS observed on heating and cooling (see Figure 9), is quite complex. Additional TEM studies are required to resolve it. At elevated temperatures, however, the triple lamellar is also found for this system. Figure 9 also demonstrates that the behavior is reversible; on cooling from the high temperature triple lamellar state a gradual transformation of the lamellar pattern to the same complicated scattering profiles is observed.

First Order Peak Disappearance. Figure 9 is a typical example of the SAXS patterns obtained from the complexes during a heat−cool-heat scan. An interesting feature, which is immediately recognized from these scans, is that the intensity of the first order peak is strongly temperature dependent and the peak even nearly disappears in some temperature interval, while the higher order peaks remain visible. This particular sample shows a rather complicated phase behavior as a function of temperature and additional efforts are required to fully resolve it. For complex **2**, the

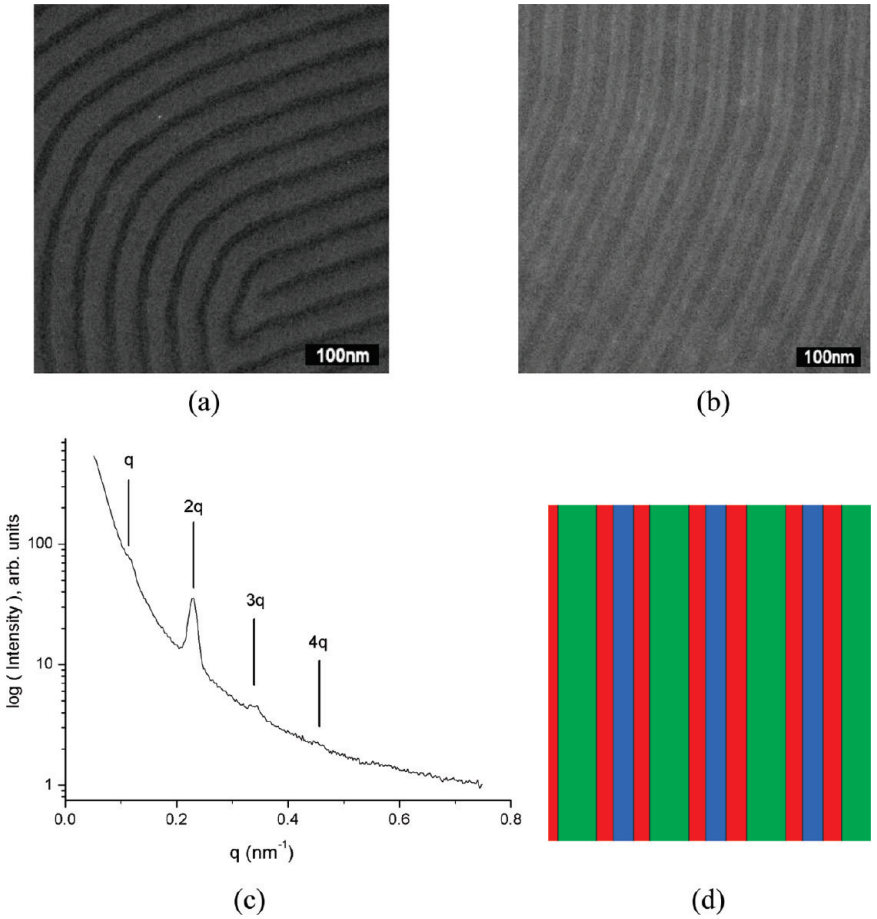

Figure 7. Bright-field TEM image of the complex **2** (Table 2), stained with iodine (a) and stained with iodine and ruthenium tetroxide (b), the corresponding SAXS intensity profile (c), and a schematic representation of the morphology (d). Green represents $P4VP(PDP)_{1.0}$, red is PS, and blue is P*t*BOS. The additional short length scale ordering in the P4VP(PDP) layers is not indicated.

temperature dependence of the scattering patterns is less involved. In this case the peak intensities also strongly change with temperature, but at all these temperatures only a lamellar morphology is observed. More interestingly, the first order scattering peak even fully disappears in a certain temperature range. To study the vanishing first order scattering peak in more detail triblock copolymer **2** (Table 1) was complexed with different amounts of PDP, ranging from r = 0.5 to 1.5, where r denotes the ratio between the numbers of PDP molecules and 4VP units. Table 3 lists the composition of these complexes, assuming that all PDP resides with the P4VP. The temperature dependent scattering patterns for the triblock copolymer 2 (Table 1) complexes with r = 0.5, 0.7, 1.0, and 1.5 are shown in Figure 10.

Whereas the pure triblock copolymer has a core−shell cylindrical self-assembled morphology, all complexes with $0.5 \leq r \leq 1.5$ form a self-assembled triple lamellar morphology. For both the pure triblock copolymer and for these complexes the morphology remains the same throughout the temperature range 0 - 200 °C investigated. The scattering curves presented show that the first order scattering peak disappears for all complexes in certain temperature intervals, depending on the amount r of PDP added. Figure 11 gives a schematic overview of the effect of r on the presence of the first order peak. It should be realized, however, that it is obviously impossible to define the vanishing of the peak unambiguously.

It appears that under certain conditions the electron density distribution within the self-assembled state is such that it becomes possible for the first order scattering peak to disappear (see Appendix A). The results summarized in Figure 11 show that once this condition is met it remains satisfied over a temperature range of several tens of degrees. It is believed to be characteristic for our unique systems involving hydrogen-bonded PDP. As discussed before, although most of the PDP will be present in the P4VP phase, some amount of PDP, strongly depending on the temperature, can also diffuse into the other domains, notably in the PS ones. More specifically, as mentioned before, it is well-known that above a certain temperature (ca. 120 °C), PDP becomes fully miscible with PS, whereas below this temperature it acts as a plasticizer. Of course, due to the favorable hydrogen bonding between P4VP and PDP most of the PDP will reside in the P4VP containing domains even at elevated temperatures. However, upon heating gradually more and more PDP will diffuse into the PS domains. It can not be excluded that a small amount of PDP will also be present in the P*t*BOS domains, although mixtures of PDP and homopolymer P*t*BOS turn out to be macrophase separated throughout the temperature range investigated . At any rate at sufficiently high temperatures a change in temperature induces a redistribution of PDP across the different domains with a corresponding change in the electron densities and, what is equally important, the layer thicknesses. Additionally, around room temperature on cooling the alkyl tails of PDP crystallize (see Figure 5) with a concurrent change in the electron density distribution inside the P4VP(PDP) layers. This explains the appearance/disappearance of the first order scattering peak at low temperatures. For instance, for r = 1.0, 1.1, and 1.2, the first order scattering peak is present above 20 °C and absent below 20 °C. For r = 0.8, on the other hand, the peak is absent above 20 °C and present below 20 °C.

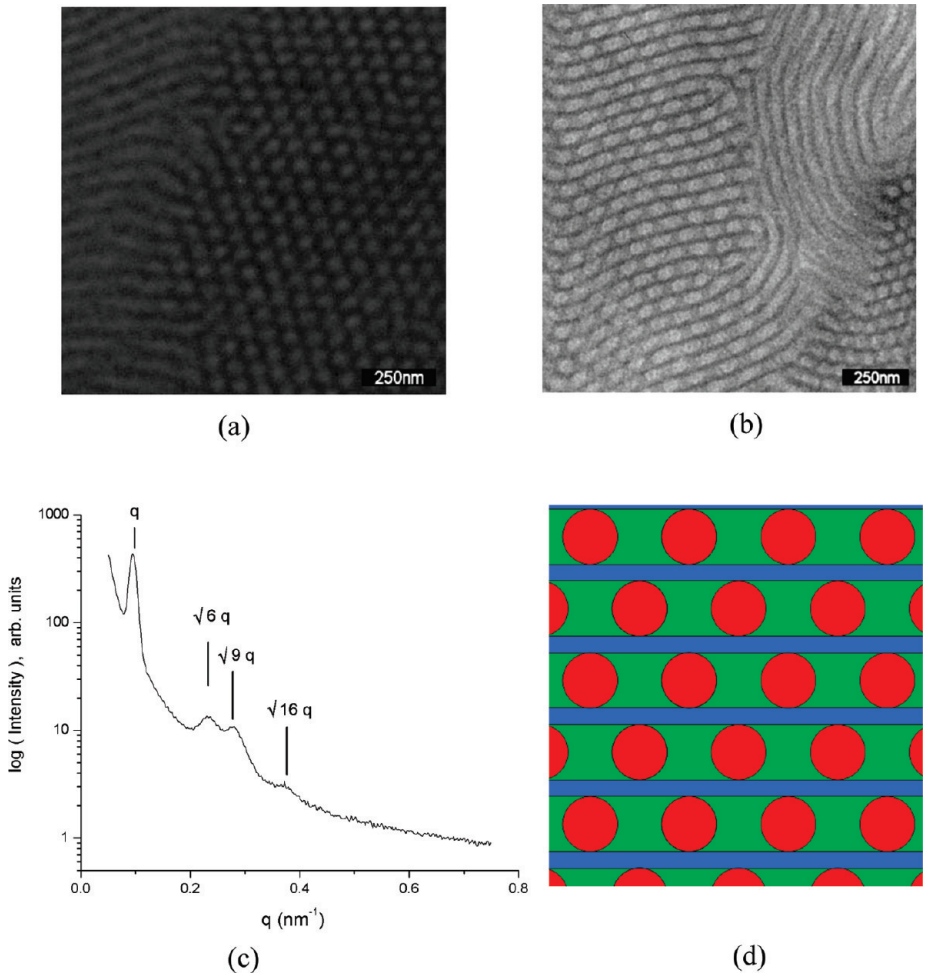

Figure 8. Bright-field TEM image of complex **4** (Table 2), stained with iodine (a) and stained with ruthenium tetroxide (b), the corresponding SAXS intensity profile at room temperature (c) and a schematic representation of the morphology (d). Green represents P4VP(PDP)$_{1.0}$, red is PS, and blue is P*t*BOS. The additional short length scale ordering in the P4VP(PDP) domains is not indicated.

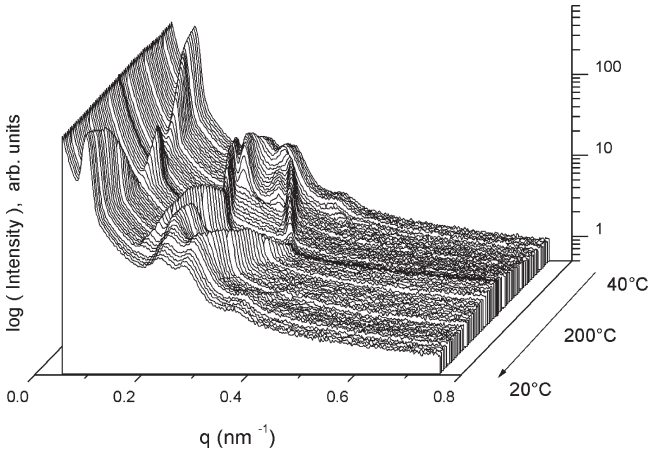

Figure 9. SAXS scattering pattern of complex **4** (Table 2) as a function of temperature during heating and cooling. To guide the eye, the scattering curve for $T = 200$ °C is bold.

Conclusions

Four different P*t*BOS-*b*-PS-*b*-P4VP linear triblock copolymers were synthesized and their self-assembly was studied with SAXS and TEM. The P4VP weight fraction varied from 0.08 to 0.39. A random copolymer study was used to determine the values of the two unknown interaction parameters as

Table 3. Composition of P*t*BOS-*b*-PS-*b*-P4VP(PDP)$_r$ Supramolecules for Triblock Copolymer 2

r	f_{tBOS}	f_{St}	$f_{4VP(PDP)r}$
0	0.29	0.56	0.15
0.5	0.19	0.58	0.24
0.6	0.18	0.56	0.26
0.7	0.18	0.54	0.28
0.8	0.17	0.53	0.30
0.9	0.17	0.52	0.31
1.0	0.16	0.50	0.33
1.1	0.16	0.49	0.35
1.2	0.16	0.48	0.36
1.3	0.15	0.47	0.38
1.4	0.15	0.46	0.39
1.5	0.15	0.45	0.40

$0.031 < \chi_{S,tBOS} < 0.034$ and $0.39 < \chi_{4VPt,BOS} < 0.43$, the latter being slightly larger than the $0.30 < \chi_{S,4VP} < 0.35$ already known from a previous study. Given these values, it was not a big surprise to find that all four systems self-assembled in the form of a P4VP/PS core/shell cylindrical morphology. Subsequently the hydrogen-bonded supramolecular complexes of P*t*BOS-*b*-PS-*b*-P4VP with stoichiometric amounts of the low molecular weight amphiphile PDP, i.e., one PDP molecule per 4VP unit, were prepared and investigated. Three of the four showed a triple lamellar morphology, with additional short length scale ordering inside the P4VP(PDP) layers. The ordered state of the sample based on the triblock

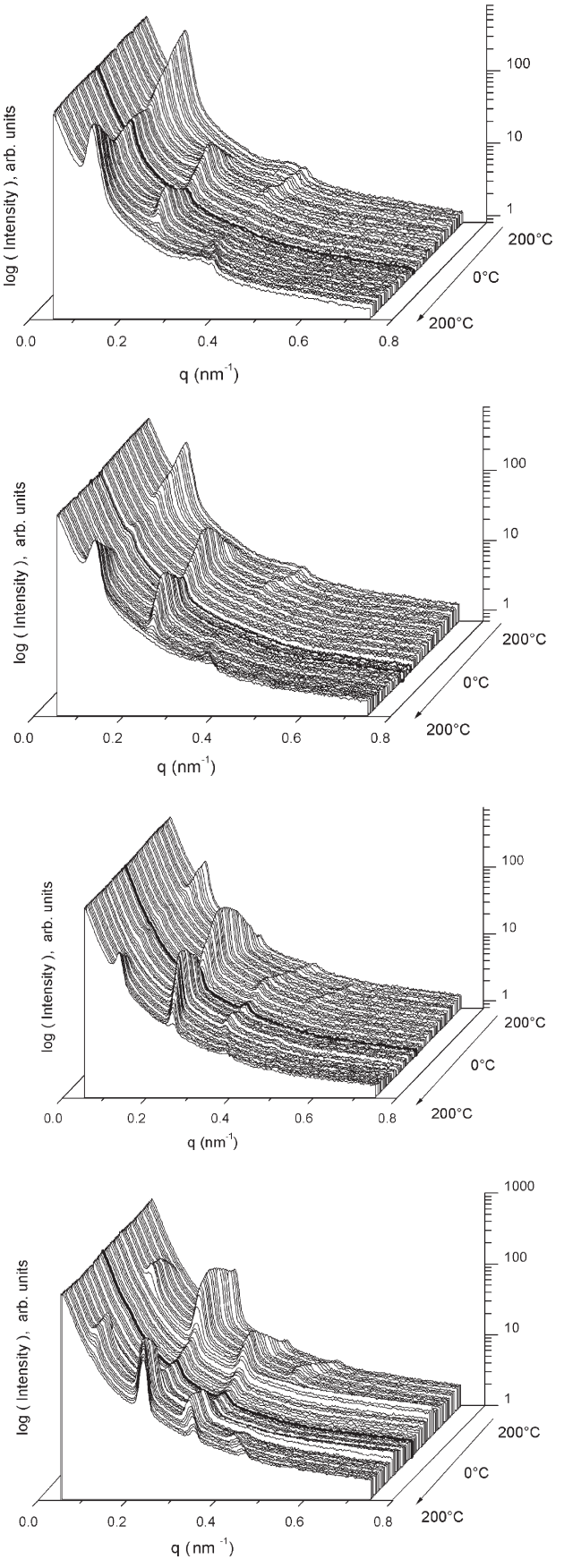

Figure 10. Temperature-dependent SAXS intensity curves for P*t*BOS-*b*-PS-*b*-P4VP(PDP)$_r$ for triblock copolymer **2**. From top to bottom: r = 0.5, r = 0.7, r = 1.0, and r = 1.5 For clarity, the curves at 0 °C are bold.

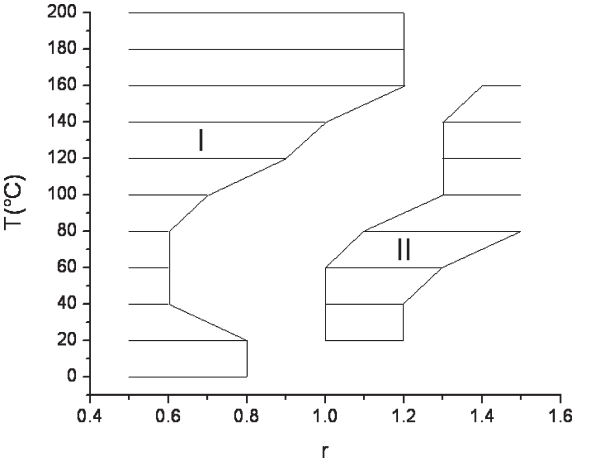

Figure 11. Presence of the first order peak for different amounts of PDP (r) as a function of temperature. In regions I and II, the first order peak is clearly observed.

copolymer with the highest fraction of P4VP consisted of alternating layers of P*t*BOS and P4VP(PDP) with PS cylinders inside the latter layer. The change in morphology is due to two effects. The presence of PDP changes the effective composition and reduces the interfacial tension between the PS- and P4VP-(PDP) domains. Another interesting feature is the disappearance of the first order scattering peak of the triple lamellar morphologies observed in certain temperature intervals, while the higher order peaks (including the third order) remain visible. We argue that this is due to the thermal sensitivity of the hydrogen bonding. On increasing the temperature, a redistribution of PDP over the different domains takes place thus changing the layer thicknesses as well as the electron density.

Acknowledgment. Janne Ruokolainen is acknowledged for valuable discussions on the TEM results. Alexander Semenov is acknowledged for a discussion on the systematic absence of first order scattering peaks. Beam time on the DUBBLE beamline of ESRF (Grenoble, France) has kindly been made available by The Netherlands Organization for Scientific Research (NWO) and we acknowledge Wim Bras and Kristina Kvashnina for experimental assistance and discussions.

Appendix A: Influence of Variable Electron Densities on the First Order Scattering Peak Intensity

In general, the absence of the first order scattering peak in a lamellar self-assembled system requires at least three different layers. The intensity of scattered X-rays is equal to the absolute square of the scattering amplitude. Therefore, if the intensity for a certain value of q is zero, the amplitude $A(q)$ is zero as well. Now,

$$A(q) = \int_V \rho(r) e^{-iqr} \, dr \qquad (1)$$

Here $\rho(r)$ denotes the scattering length density distribution, which for X-rays is proportional to the electron density distribution.[55] To show how this might become zero, we consider three layers with an scattering length density or electron density distribution as drawn schematically in Figure 12.

Here we consider the situation that the electron density of the middle red block is lower than the electron densities of the end blue and green blocks. Since only the electron density difference is important and not the absolute value, we may choose the electron density of the red block to be zero. Accordingly, the electron densities of the A (blue) and C block (green) are of the same sign.

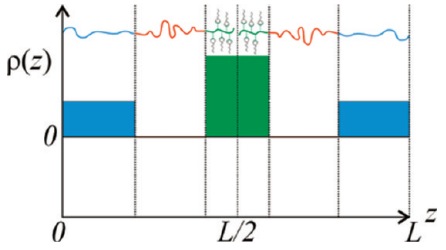

Figure 12. Schematic representation of the lamellar self-assembly and the scattering length density profile $\rho(z)$.

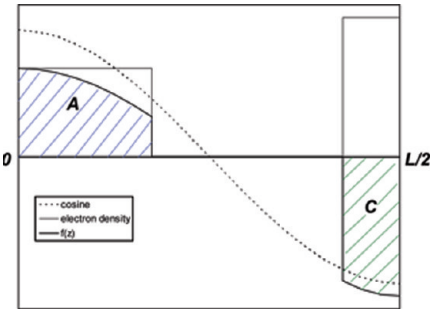

Figure 13. Scattering length density distribution $\rho(z)$, $\cos(2\pi z/L)$ and $f(z) = \rho(z)\cos(2\pi z/L)$ for half the period of a triple lamellar structure.

Furthermore, without loss of generality, we may define A and C such that the latter has the highest electron density. In this kind of situation the first order peak may easily be absent. It is also the situation encountered by Ludwigs et al.[56] for their polystyrene-*b*-poly(2-vinylpyridine)-*b*-poly(*tert*-butyl methacrylate) triblock copolymers. They actually estimated the absolute electron densities of the blocks and indeed found the middle block to have the lowest electron density. Note that due to the distribution of PDP through the different domains, it is much more difficult to estimate absolute electron densities in our case. Applying eq 1 to the situation sketched in Figure 12 gives

$$A(q) = \int_0^{L/2} \rho(z) e^{-iqz}\, dz + \int_{L/2}^{L} \rho(z) e^{-iqz}\, dz \qquad (2)$$

Which due to the symmetry of $\rho(z)$ with respect to $z = L/2$ reduces to

$$A(q) = \int_0^{L/2} \rho(z) \cos\frac{2\pi z}{L}\, dz + \int_{L/2}^{L} \rho(z) \cos\frac{2\pi z}{L}\, dz \qquad (3)$$

Figure 13 shows $\rho(z)$, $\cos(2\pi z/L)$ as well as the product $f(z) = \rho(z)\cos(2\pi z/L)$.

This picture demonstrates that the integral of $f(z)$ over half the period becomes zero once the integral of $f(z)$ over the A domain cancels the one over the C domain. The second term in eq 3 will then be zero as well. We notice that both the electron density difference and the layer thickness have to be just right to allow for full extinction of the first order peak. Furthermore, it is easy to convince oneself that in the example sketched in Figure 12 and 13 the higher order peaks, notably the third order, will not be zero.

References and Notes

(1) Hamley, I. W., *The Physics of Block Copolymers*: Oxford University Press: Oxford, U.K., 1998.
(2) Fasolka, M. J.; Mayes, A. M. *Annu. Rev. Mater. Res.* **2001**, *31*, 323.
(3) Förster, S.; Plantenberg, T. *Angew. Chem., Int. Ed.* **2002**, *41*, 689.
(4) Park, C.; Yoon, J.; Thomas, E. L. *Polymer* **2003**, *44*, 6725.
(5) Hamley, I. W. *Angew. Chem., Int. Ed.* **2003**, *42*, 1692.
(6) Lehn, J.-M., *Supramol. Chem.*, Wiley-VCH: Weinheim, Germany, 1995.
(7) Ruokolainen, J.; Mäkinen, R.; Torkkeli, M.; Mäkelä, T.; Serimaa, R.; ten Brinke, G.; Ikkala, O. *Science* **1998**, *280*, 557.
(8) Ikkala, O.; ten Brinke, G. *Science* **2002**, *295*, 2407.
(9) Ikkala, O.; ten Brinke, G. *Chem. Commun.* **2004**, 2131.
(10) ten Brinke, G.; Ikkala, O. *Chem. Rec.* **2004**, *4*, 219.
(11) Pollino, J. M.; Weck, M. *Chem. Soc. Rev.* **2005**, *34*, 193.
(12) Valkama, S.; Kosonen, H.; Ruokolainen, J.; Torkkeli, M.; Serimaa, R.; ten Brinke, G.; Ikkala, O. *Nat. Mater.* **2004**, *3*, 872.
(13) Mäkinen, R.; de Moel, K.; de Odorico, W.; Ruokolainen, J.; Stamm, M.; ten Brinke, G.; Ikkala, O. *Adv. Mater.* **2001**, *13*, 107.
(14) de Moel, K.; Alberda van Ekenstein, G. O. R.; Nijland, H.; Polushkin, E.; ten Brinke, G.; Mäki-Ontto, R.; Ikkala, O. *Chem. Mater.* **2001**, *13*, 4580.
(15) Fahmi, A. W.; Gutmann, J. S.; Vogel, R.; Gindy, N.; Stamm, M. *Macromol. Mater. Eng.* **2006**, *291*, 1061.
(16) Liu, X.; Stamm, M. *Nanoscale Res. Lett.* **2009**, *4*, 459.
(17) Hillmyer, M. A. *Adv. Polym. Sci.* **2005**, *190*, 137.
(18) Peinemann, K.-V.; Abetz, V.; Simon, P. F. W. *Nat. Mater.* **2007**, *6*, 992.
(19) Hashimoto, T.; Nishikawa, Y.; Tsutsumi, K. *Macromolecules* **2007**, *40*, 1066.
(20) Mao, H.; Hillmyer, M. A. *Soft Matter* **2006**, *2*, 57.
(21) Zalusky, A. S.; Olayo-Valles, R.; Wolf, J. H.; Hillmyer, M. A. *J. Am. Chem. Soc.* **2002**, *124*, 12761.
(22) Peinemann, K.-V.; Abetz, V.; Simon, P. F. W. *Nat. Mater.* **2007**, *6*, 992.
(23) Urbas, A. M.; Maldovan, M.; DeRege, P.; Thomas, E. L. *Adv. Mater.* **2002**, *14*, 1850.
(24) Park, S.; Wang, J. Y.; Kim, B.; Xu, J.; Russell, T. P. *Nano* **2008**, *2*, 766.
(25) Crossland, E. J. W.; Kamperman, M.; Nedelcu, M.; Ducati, C.; Wiesner, U.; Smilgies, D. M.; Toombes, G. E. S.; Hillmyer, M. A.; Ludwigs, S.; Steiner, U.; Snaith, H. J. *Nano Lett.* **2009**, *9*, 2807.
(26) Joo, W.; Yang, S. Y.; Kim, J. K.; Jinnai, H. *Langmuir* **2008**, *24*, 12612.
(27) Mansky, P.; Harrison, C. K.; Chaikin, P. M.; Register, R. A.; Yao, N. *Appl. Phys. Lett.* **1996**, *68*, 2586.
(28) Chen, S. Y.; Huang, Y.; Tsiang; Chien-Chao, R. *J. Pol. Sci., Part A: Polym. Chem.* **2008**, *46*, 1964.
(29) Bates, F. S.; Fredrickson, G. H. *Phys. Today* **1999**, *52*, 32.
(30) Mogi, Y.; Mori, K.; Kotsuji, H.; Matsushita, Y.; Noda, I.; Han, C. C. *Macromolecules* **1993**, *26*, 5169.
(31) Mogi, Y.; Nomura, M.; Kotsuji, H.; Ohnishi, K.; Matsushita, Y.; Noda, I. *Macromolecules* **1994**, *27*, 6755.
(32) Bailey, T. S.; Pham, H. D.; Bates, F. S. *Macromolecules* **2001**, *34*, 6994.
(33) Balsamo, V.; Stadler, R. *Macromol. Symp.* **1997**, *117*, 153.
(34) Brinkmann, S.; Stadler, R.; Thomas, E. L. *Macromolecules* **1995**, *28*, 6566.
(35) Krappe, U.; Stadler, R.; Voigt-Martin, I. *Macromolecules* **1995**, *28*, 4558.
(36) Stadler, R.; Auschra, C.; Beckmann, J.; Krappe, U.; Voight-Martin, I.; Leibler, L. *Macromolecules* **1995**, *28*, 3080.
(37) Breiner, U.; Krappe, U.; Thomas, E. L.; Stadler, R. *Macromolecules* **1998**, *31*, 135.
(38) Tyler, C. A.; Qin, J.; Bates, F. S.; Morse, D. C. *Macromolecules* **2007**, *40*, 4654.
(39) Alberda van Ekenstein, G. O. R.; Meyboom, R.; ten Brinke, G.; Ikkala, O. *Macromolecules* **2000**, *33*, 3752.
(40) Gobius du Sart, G. *Supramolecular Triblock Copolymer Complexes*; Thesis, Groningen University 2009; http://irs.ub.rug.nl/ppn/317892029.
(41) Polushkin, E.; Alberda van Ekenstein, G. O. R.; Knaapila, M.; Ruokolainen, J.; Torkkeli, M.; Serimaa, R.; Bras, W.; Dolbnya, I.; Ikkala, O.; ten Brinke, G. *Macromolecules* **2001**, *34*, 4917.
(42) Bras, W.; Dolbnya, I. P.; Detollenaere, D.; van Tol, R.; Malfois, M.; Greaves, G. N.; Ryan, A. J.; Heeley, E. *J. Appl. Crystallogr.* **2003**, *36*, 791.
(43) Zha, W.; Han, C. D.; Lee, D. H.; Han, S. H.; Kim, J. K.; Kang, J. H.; Park, C. *Macromolecules* **2007**, *40*, 2109.
(44) Matsushita, Y.; Yamada, K.; Hattori, T.; Fujimoto, T.; Sawada, Y.; Nagasawa, M.; Matsui, C. *Macromolecules* **1983**, *16*, 10.

(45) Takashi, K.; Hasegawa, H.; Hashimoto, T. *Macromolecules* **2002**, *35*, 4859.
(46) Gido, S. P.; Schwark, D. W.; Thomas, E. L. *Macromolecules* **1993**, *26*, 2636.
(47) Chatterjee, J.; Jain, S.; Bates, F. S. *Macromolecules* **2007**, *40*, 2882.
(48) Tang, P.; Qiu, F.; Zhang, H.; Yang, Y. *Phys. Rev. E* **2004**, *69*, 031803.
(49) van Zoelen, W.; Alberda van Ekenstein, G.; Ikkala, O.; ten Brinke, G. *Macromolecules* **2006**, *39*, 6574.
(50) Ruokolainen, J.; ten Brinke, G.; Ikkala, O.; Torkkeli, M.; Serimaa, R. *Macromolecules* **1996**, *29*, 3409.
(51) Ruokolainen, J.; Torkkeli, M.; Serimaa, R.; Komanschek, B. E.; Ikkala, O.; ten Brinke, G. *Phys. Rev. E.* **1996**, *54*, 6646.
(52) Ruokolainen, J.; Saariaho, M.; Ikkala, O.; ten Brinke, G.; Thomas, E. L.; Torkkeli, M.; Serimaa, R. *Macromolecules* **1999**, *32*, 1152.
(53) Eichhorn, K.-J.; Fahmi, A.; Adam, G.; Stamm, M. *J. Mol. Struct.* **2003**, *661*−*662*, 161.
(54) Milner, S. T. *Macromolecules* **1994**, *27*, 2333.
(55) Roe, R.-J. *Methods of X-Ray and Neutron Scattering in Polymer Science*; Oxford University Press: Oxford, NY, 2000.
(56) Ludwigs, S.; Böker, A.; Abetz, V.; Müller, A. H. E.; Krausch, G. *Polymer* **2003**, *44*, 6815.